Supplementary Materials

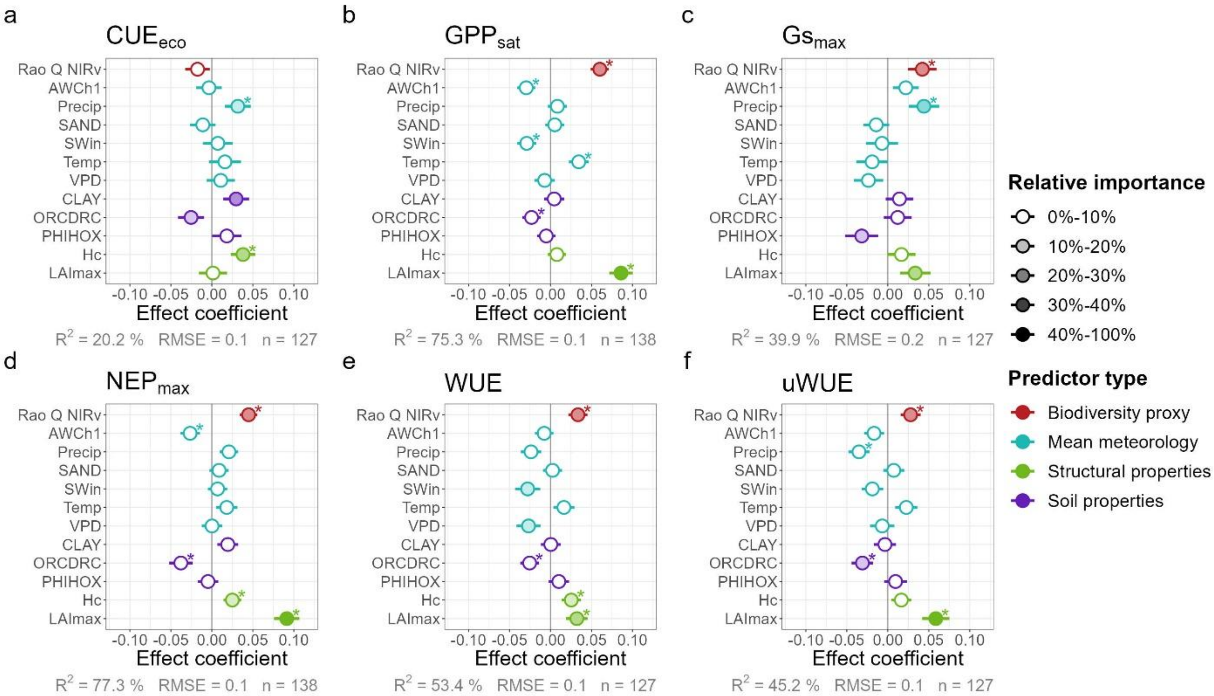

Figure S1. Effect coefficients from multimodel inference predictions of ecosystem functional properties. Colours indicate the category of the predictor variable, while transparency represents the values of relative importance for each predictor variable. Asterisks indicate significant effects (*p*-value < 0.05). Captions to each subplot present the fraction of variance explained by the model (R^2), the root mean square error (RMSE), and the number of sites included in each model ensemble (n). Variable acronyms: i) Response variables: ecosystem carbon use-efficiency (CUE_{eco}), photosynthetic capacity at light saturation (GPP_{sat}), surface conductance (Gs_{max}), maximum net ecosystem productivity (NEP_{max}), water use-efficiency (WUE), underlying water use-efficiency (uWUE); ii) predictor variables: Rao Q calculated from near-infrared reflectance of vegetation (Rao Q NIRv), precipitation (Precip), incoming shortwave radiation (SWin), air temperature (Temp), vapor pressure deficit (VPD), maximum vegetation height (Hc), maximum leaf area index (LAImax), relative clay content (CLAY), soil organic carbon content (fine earth fraction, ORCDRC), Soil pH x 10 in water (PHIHOX).

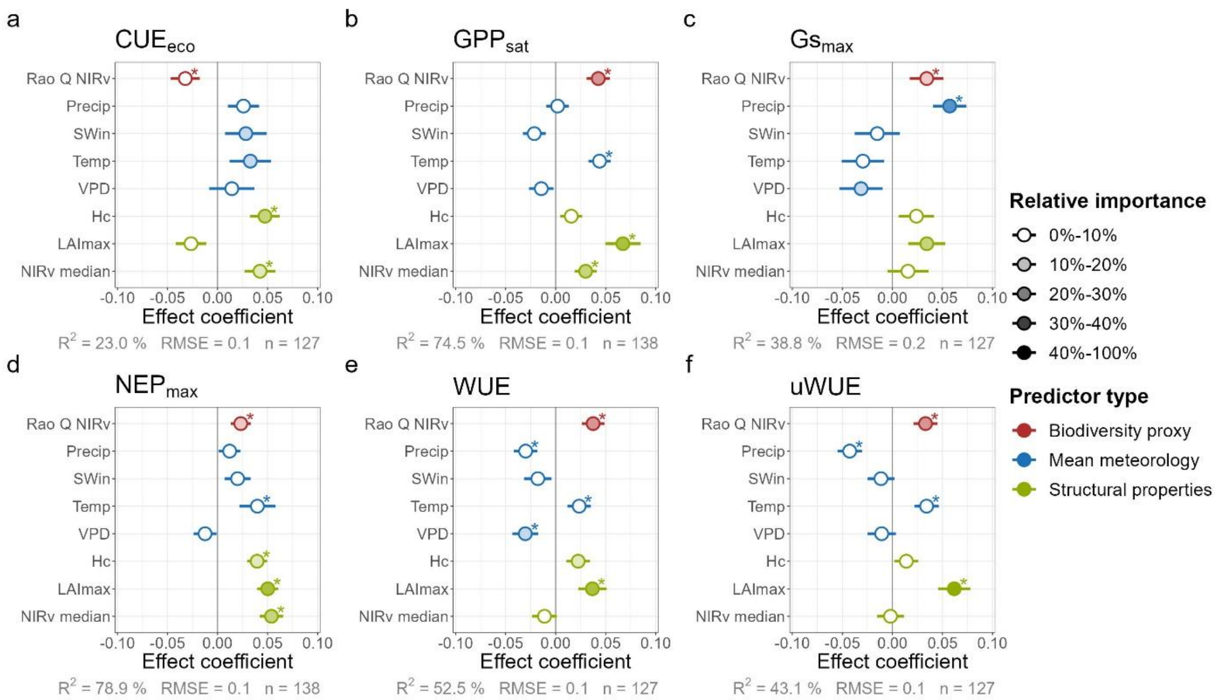

Figure S2. Effect coefficients from multimodel inference predictions of ecosystem functional properties. Colours indicate the category of the predictor variable, while transparency represents the values of relative importance for each predictor variable. Asterisks indicate significant effects (*p*-value < 0.05). Captions to each subplot present the fraction of variance explained by the model (R^2), the root mean square error (RMSE), and the number of sites included in each model ensemble (n). Variable acronyms: i) Response variables: ecosystem carbon use-efficiency (CUE_{eco}), photosynthetic capacity at light saturation (GPP_{sat}), surface conductance (Gs_{max}), maximum net ecosystem productivity (NEP_{max}), water use-efficiency (WUE), underlying water use-efficiency (uWUE); ii) predictor variables: Rao Q calculated from near-infrared reflectance of vegetation (Rao Q NIRv), precipitation (Precip), incoming shortwave radiation (SWin), air temperature (Temp), vapor pressure deficit (VPD), maximum vegetation height (Hc), maximum leaf area index (LAImax), median near-infrared reflectance of vegetation (NIRv median).

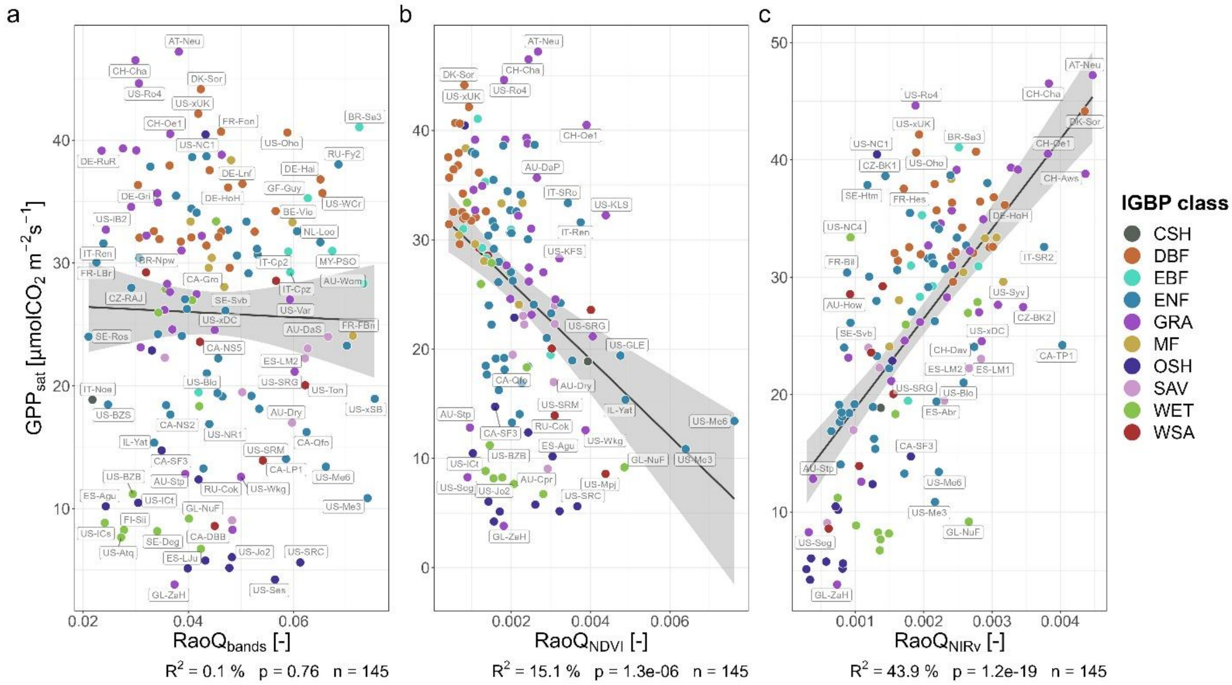

Figure S3. Bivariate relationships between photosynthetic capacity at light saturation (GPP_{sat}) and Rao Q metrics computed from all bands and vegetation indices derived from Sentinel-2. a. GPP_{sat} vs $RaoQ_{bands}$. b. GPP_{sat} vs $RaoQ_{NDVI}$. c. GPP_{sat} vs $RaoQ_{NIRv}$. Marker colours represent plant functional types following the IGBP classification: Closed Shrubland (CSH), Deciduous Broadleaf Forests (DBF), Evergreen Broadleaf Forests (EBF), Evergreen Needleleaf Forests (ENF), Grasslands (GRA), Mixed Forests (MF), Open Shrublands (OSH), Savannas (SAV), Permanent Wetlands (WET), Woody Savannas (WSA). Labels refer to the site IDs (see Table S2).

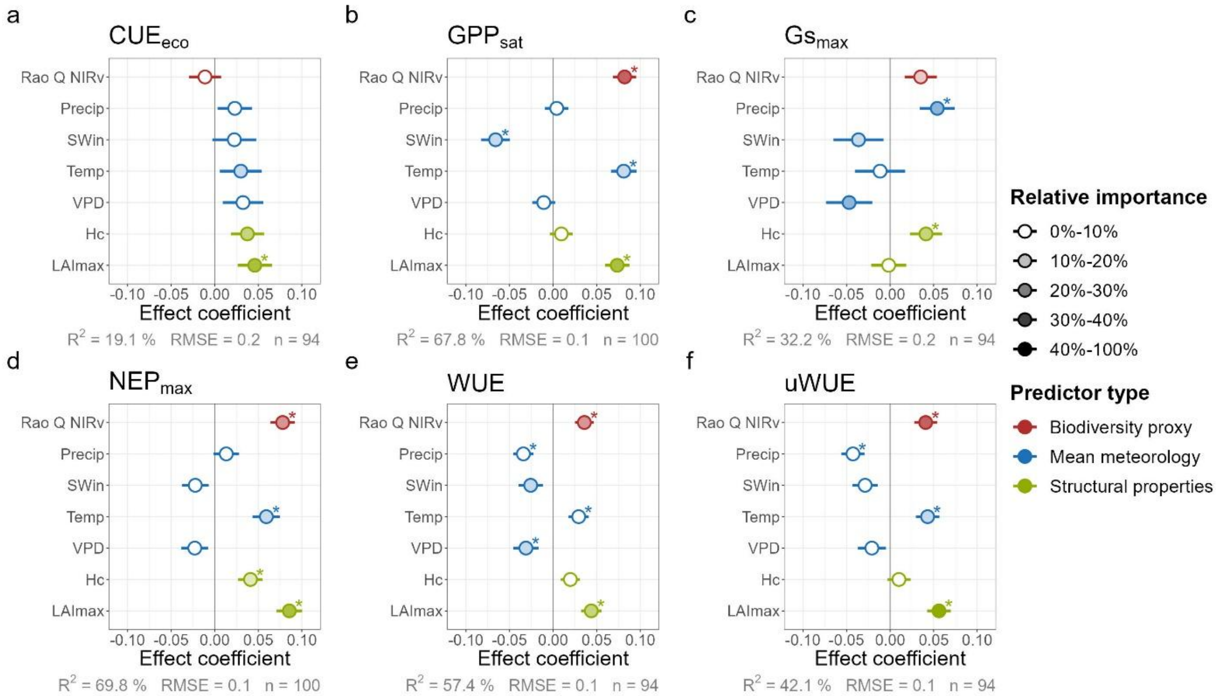

Figure S4. Effect coefficients from multimodel inference predictions of ecosystem functional properties. Colours indicate the category of the predictor variable, while transparency represents the values of relative importance for each predictor variable. Asterisks indicate significant effects (*p*-value < 0.05). Captions to each subplot present the fraction of variance explained by the model (R^2), the root mean square error (RMSE), and the number of sites included in each model ensemble (n). Variable acronyms: i) Response variables: ecosystem carbon use-efficiency (CUE_{eco}), photosynthetic capacity at light saturation (GPP_{sat}), surface conductance (Gs_{max}), maximum net ecosystem productivity (NEP_{max}), water use-efficiency (WUE), underlying water use-efficiency (uWUE); ii) predictor variables: Rao Q calculated from near-infrared reflectance of vegetation (Rao Q NIRv), precipitation (Precip), incoming shortwave radiation (SWin), air temperature (Temp), vapor pressure deficit (VPD), maximum vegetation height (Hc), maximum leaf area index from ground measurements (LAImax).

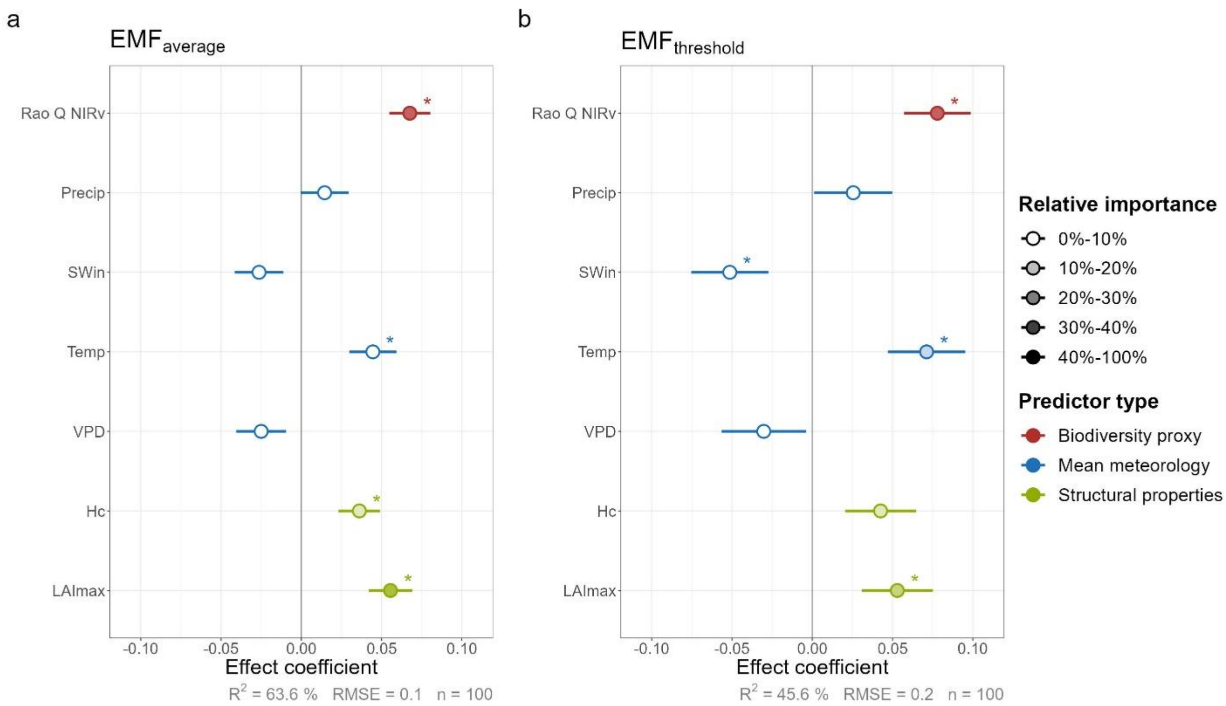

Figure S5. Effect coefficients from multimodel inference predictions of ecosystem functional properties. Colours indicate the category of the predictor variable, while transparency represents the values of relative importance for each predictor variable. Asterisks indicate significant effects (*p*-value < 0.05). Captions to each subplot present the fraction of variance explained by the model (R^2), the root mean square error (RMSE), and the number of sites included in each model ensemble (n). Variable acronyms: i) Response variables: average ecosystem multifunctionality ($EMF_{average}$), threshold ecosystem multifunctionality ($EMF_{threshold}$); ii) predictor variables: Rao Q calculated from near-infrared reflectance of vegetation (Rao Q NIRv), precipitation (Precip), incoming shortwave radiation (SWin), air temperature (Temp), vapor pressure deficit (VPD), maximum vegetation height (Hc), maximum leaf area index from ground measurements (LAImax).

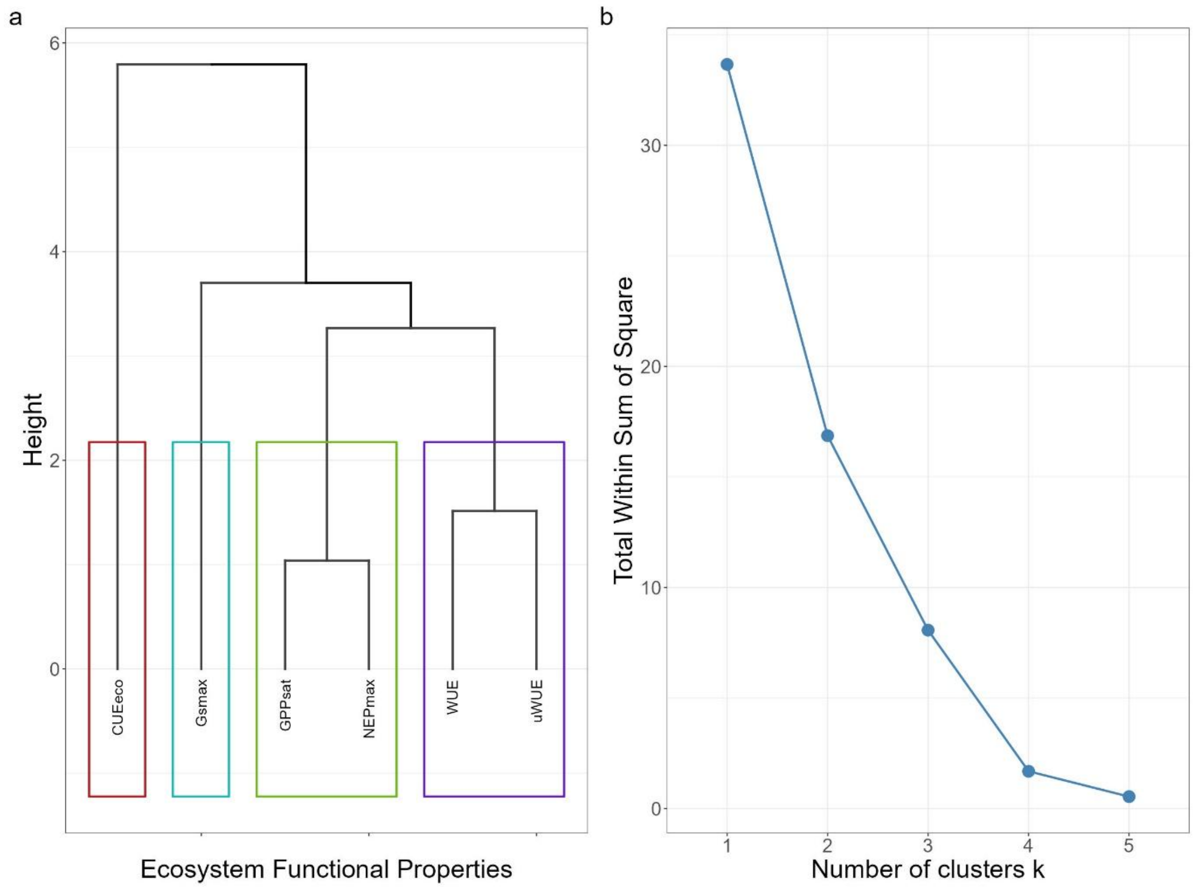

Figure S6. Hierarchical clustering analysis results. a. Dendrogram of ecosystem functional properties. Coloured boxes indicate the clusters resulting from agglomerative hierarchical cluster analysis. Acronyms: ecosystem carbon use-efficiency (CUEeco), photosynthetic capacity at light saturation (GPPsat), surface conductance (Gsmax), maximum net ecosystem productivity (NEPmax), water use-efficiency (WUE), underlying water use-efficiency (uWUE). b. Total within cluster sum of squares *vs* number of clusters k.

Table S1. Weighted statistics for each prediction model. Model refers to the set of models used to predict the specified variable; variable lists the predictors, R^2 is the explained variance of the model, AICc the second-order Akaike Information Criterion, $RMSE_{full}$ the Root Mean Square Error of the multimodel inference, $RMSE_{loo}$ refers to the leave-one-out cross-validation RMSE, rel shows the relative importance values for each predictor, n is the number of datapoints included in the models (note that n is different based on available data for the for different set of predicted and predictor variables), coef refers to the predictor average coefficient, se is the standard error, adj se the adjusted standard error, z val refers to the Z statistics, and p val to the average model *p*-value. Values are obtained via weighted averages based on weights outputted by the multimodel inference analysis.

model	variable	R^2	AICc	$RMSE_{full}$	$RMSE_{loo}$	rel	n	coef	se	adj se	z val	p val
CUEeco	Temp	0.16	-98.34	0.16	0.17	33.4%	127	0.04	0.02	0.02	1.73	0.08
CUEeco	Hc	0.16	-98.34	0.16	0.17	32.9%	127	0.04	0.01	0.01	2.59	0.01
CUEeco	Precip	0.16	-98.34	0.16	0.17	14.8%	127	0.03	0.02	0.02	1.62	0.10
CUEeco	SWin	0.16	-98.34	0.16	0.17	10.7%	127	0.02	0.02	0.02	1.09	0.28
CUEeco	VPD	0.16	-98.34	0.16	0.17	6.8%	127	0.02	0.02	0.02	0.77	0.44
CUEeco	LAImax	0.16	-98.34	0.16	0.17	0.7%	127	0.00	0.02	0.02	0.08	0.93
CUEeco	Rao_Q_NIRv	0.16	-98.34	0.16	0.17	0.6%	127	-0.01	0.01	0.01	0.76	0.45
GPPsat	LAImax	0.73	-171.68	0.12	0.13	54.0%	138	0.10	0.01	0.01	6.99	0.00
GPPsat	Rao_Q_NIRv	0.73	-171.68	0.12	0.13	30.2%	138	0.06	0.01	0.01	5.66	0.00
GPPsat	Temp	0.73	-171.68	0.12	0.13	7.0%	138	0.04	0.01	0.01	3.92	0.00
GPPsat	SWin	0.73	-171.68	0.12	0.13	4.4%	138	-0.02	0.01	0.01	1.92	0.05
GPPsat	VPD	0.73	-171.68	0.12	0.13	2.2%	138	-0.01	0.01	0.01	0.92	0.36
GPPsat	Hc	0.73	-171.68	0.12	0.13	1.2%	138	0.00	0.01	0.01	0.38	0.71
GPPsat	Precip	0.73	-171.68	0.12	0.13	1.1%	138	0.00	0.01	0.01	0.18	0.86
Gsmax	Precip	0.39	-87.85	0.16	0.17	30.4%	127	0.06	0.02	0.02	3.39	0.00
Gsmax	LAImax	0.39	-87.85	0.16	0.17	25.7%	127	0.04	0.02	0.02	2.01	0.04
Gsmax	Rao_Q_NIRv	0.39	-87.85	0.16	0.17	19.6%	127	0.04	0.02	0.02	2.17	0.03
Gsmax	VPD	0.39	-87.85	0.16	0.17	11.9%	127	-0.03	0.02	0.02	1.41	0.16
Gsmax	Hc	0.39	-87.85	0.16	0.17	5.2%	127	0.02	0.02	0.02	1.21	0.23
Gsmax	Temp	0.39	-87.85	0.16	0.17	3.9%	127	-0.03	0.02	0.02	1.40	0.16
Gsmax	SWin	0.39	-87.85	0.16	0.17	3.2%	127	-0.02	0.02	0.02	0.69	0.49
NEPmax	LAImax	0.74	-173.82	0.12	0.13	52.6%	138	0.11	0.02	0.02	6.36	0.00
NEPmax	Rao_Q_NIRv	0.74	-173.82	0.12	0.13	23.6%	138	0.05	0.01	0.01	4.59	0.00
NEPmax	Hc	0.74	-173.82	0.12	0.13	10.2%	138	0.02	0.01	0.01	1.99	0.05
NEPmax	Temp	0.74	-173.82	0.12	0.13	8.1%	138	0.05	0.02	0.02	2.32	0.02
NEPmax	Precip	0.74	-173.82	0.12	0.13	3.1%	138	0.01	0.01	0.01	0.97	0.33
NEPmax	VPD	0.74	-173.82	0.12	0.13	1.3%	138	-0.01	0.01	0.01	0.43	0.67
NEPmax	SWin	0.74	-173.82	0.12	0.13	1.1%	138	0.02	0.01	0.01	1.19	0.23
uWUE	LAImax	0.43	-146.43	0.13	0.14	50.8%	127	0.06	0.02	0.02	4.04	0.00
uWUE	Rao_Q_NIRv	0.43	-146.43	0.13	0.14	26.9%	127	0.03	0.01	0.01	2.79	0.01
uWUE	Precip	0.43	-146.43	0.13	0.14	6.8%	127	-0.04	0.01	0.01	3.46	0.00
uWUE	Temp	0.43	-146.43	0.13	0.14	6.1%	127	0.03	0.01	0.01	2.79	0.01
uWUE	Hc	0.43	-146.43	0.13	0.14	5.7%	127	0.01	0.01	0.01	1.15	0.25

uWUE	VPD	0.43	-146.43	0.13	0.14	2.0%	127	-0.01	0.01	0.01	0.75	0.45
uWUE	SWin	0.43	-146.43	0.13	0.14	1.7%	127	-0.01	0.01	0.01	0.85	0.40
WUE	LAImax	0.52	-174.41	0.11	0.12	32.9%	127	0.04	0.01	0.01	2.63	0.01
WUE	Rao_Q_NIRv	0.52	-174.41	0.11	0.12	24.1%	127	0.04	0.01	0.01	3.26	0.00
WUE	VPD	0.52	-174.41	0.11	0.12	19.2%	127	-0.03	0.01	0.01	2.39	0.02
WUE	Hc	0.52	-174.41	0.11	0.12	11.5%	127	0.02	0.01	0.01	2.08	0.04
WUE	Temp	0.52	-174.41	0.11	0.12	4.7%	127	0.02	0.01	0.01	2.00	0.05
WUE	SWin	0.52	-174.41	0.11	0.12	3.8%	127	-0.02	0.01	0.01	1.25	0.21
WUE	Precip	0.52	-174.41	0.11	0.12	3.8%	127	-0.03	0.01	0.01	2.54	0.01
EMFavg	LAImax	0.66	-189.67	0.12	0.12	47.3%	138	0.07	0.01	0.01	4.67	0.00
EMFavg	Rao_Q_NIRv	0.66	-189.67	0.12	0.12	27.8%	138	0.05	0.01	0.01	4.65	0.00
EMFavg	Hc	0.66	-189.67	0.12	0.12	10.4%	138	0.02	0.01	0.01	2.04	0.04
EMFavg	Temp	0.66	-189.67	0.12	0.12	6.0%	138	0.03	0.01	0.01	2.88	0.00
EMFavg	VPD	0.66	-189.67	0.12	0.12	4.4%	138	-0.02	0.01	0.01	1.46	0.14
EMFavg	Precip	0.66	-189.67	0.12	0.12	3.5%	138	0.01	0.01	0.01	1.00	0.32
EMFavg	SWin	0.66	-189.67	0.12	0.12	0.6%	138	0.00	0.01	0.01	0.03	0.97
EMFthr	LAImax	0.45	-61.69	0.18	0.19	39.7%	138	0.06	0.02	0.02	2.70	0.01
EMFthr	Rao_Q_NIRv	0.45	-61.69	0.18	0.19	21.7%	138	0.04	0.02	0.02	2.60	0.01
EMFthr	Hc	0.45	-61.69	0.18	0.19	17.1%	138	0.04	0.02	0.02	2.17	0.03
EMFthr	Precip	0.45	-61.69	0.18	0.19	13.3%	138	0.04	0.02	0.02	1.92	0.05
EMFthr	Temp	0.45	-61.69	0.18	0.19	4.9%	138	0.04	0.02	0.02	1.93	0.05
EMFthr	VPD	0.45	-61.69	0.18	0.19	1.9%	138	-0.01	0.02	0.02	0.32	0.75
EMFthr	SWin	0.45	-61.69	0.18	0.19	1.6%	138	-0.02	0.02	0.02	0.77	0.44

Table S2: List of sites.

SITE_ID	IGBP	LATITUDE	LONGITUDE	DOI	SITE_NAME	DATA SOURCE
AT-Neu	GRA	47.116669	11.317500	https://doi.org/10.18140/FLX/1440121	Neustift	FLUXNET2015
AU-Cpr	SAV	-34.002100	140.589100	https://doi.org/10.18140/FLX/1440195	Calperum	FLUXNET2015
AU-DaP	GRA	-14.063300	131.318100	https://doi.org/10.18140/FLX/1440123	Daly River Savanna	FLUXNET2015
AU-DaS	SAV	-14.159300	131.388100	https://doi.org/10.18140/FLX/1440122	Daly River Cleared	FLUXNET2015
AU-Dry	SAV	-15.258800	132.370600	https://doi.org/10.18140/FLX/1440197	Dry River	FLUXNET2015
AU-How	WSA	-12.494300	131.152300	https://doi.org/10.18140/FLX/1440125	Howard Springs	FLUXNET2015
AU-Stp	GRA	-17.150700	133.350200	https://doi.org/10.18140/FLX/1440204	Sturt Plains	FLUXNET2015
AU-Wom	EBF	-37.422200	144.094400	https://doi.org/10.18140/FLX/1440207	Wombat	FLUXNET2015
BE-Bra	MF	51.307610	4.519840	https://doi.org/10.18160/2G60-ZHAK	Brasschaat	WarmWinter2020
BE-Dor	GRA	50.311928	4.968011	https://doi.org/10.18160/2G60-ZHAK	Dorinne	WarmWinter2020
BE-Maa	CSH	50.980111	5.631861	https://doi.org/10.18160/2G60-ZHAK	Maasmechelen	WarmWinter2020
BE-Vie	MF	50.304933	5.998115	https://doi.org/10.18160/2G60-ZHAK	Vielsalm	WarmWinter2020
BR-Npw	WSA	-16.498000	-56.412000	https://doi.org/10.17190/AMF/1881563	Northern Pantanal Wetland	AmerifluxFLUXNET
BR-Sa3	EBF	-3.018000	-54.971400	https://doi.org/10.18140/FLX/1440033	Santarem-Km83-Logged Forest	FLUXNET2015
CA-ARB	WET	52.695000	-83.945200	https://doi.org/10.17190/AMF/1902821	Attawapiskat River Bog	AmerifluxFLUXNET
CA-DBB	WET	49.129300	-122.984900	https://doi.org/10.17190/AMF/1881565	Delta Burns Bog	AmerifluxFLUXNET
CA-Gro	MF	48.216700	-82.155600	https://doi.org/10.17190/AMF/1902823	Ontario - Groundhog River, Boreal Mixedwood Forest	AmerifluxFLUXNET
CA-LP1	ENF	55.111900	-122.841400	https://doi.org/10.17190/AMF/1832155	British Columbia - Mountain pine beetle-attacked lodgepole pine stand	AmerifluxFLUXNET
CA-NS2	ENF	55.905800	-98.524700	https://doi.org/10.18140/FLX/1440037	UCI-1930 burn site	FLUXNET2015
CA-NS3	ENF	55.911700	-98.382200	https://doi.org/10.18140/FLX/1440038	UCI-1964 burn site	FLUXNET2015
CA-NS5	ENF	55.863100	-98.485000	https://doi.org/10.18140/FLX/1440040	UCI-1981 burn site	FLUXNET2015
CA-Oas	DBF	53.628900	-106.197800	https://doi.org/10.18140/FLX/1440043	Saskatchewan - Western Boreal, Mature Aspen	FLUXNET2015
CA-Obs	ENF	53.987200	-105.117800	https://doi.org/10.18140/FLX/1440044	Saskatchewan - Western Boreal, Mature Black Spruce	FLUXNET2015
CA-Qfo	ENF	49.692500	-74.342100	https://doi.org/10.18140/FLX/1440045	Quebec - Eastern Boreal, Mature Black Spruce	FLUXNET2015
CA-SF2	ENF	54.253900	-105.877500	https://doi.org/10.18140/FLX/1440047	Saskatchewan - Western Boreal,	FLUXNET2015

					forest burned in 1989	
CA-SF3	OSH	54.091600	-106.005300	https://doi.org/10.18140/FLX/1440048	Saskatchewan - Western Boreal, forest burned in 1998	FLUXNET2015
CA-TP1	ENF	42.660900	-80.559500	https://doi.org/10.18140/FLX/1440050	Ontario - Turkey Point 2002 Plantation White Pine	FLUXNET2015
CA-TP4	ENF	42.710200	-80.357400	https://doi.org/10.18140/FLX/1440053	Ontario - Turkey Point 1939 Plantation White Pine	FLUXNET2015
CA-TPD	DBF	42.635300	-80.557700	https://doi.org/10.17190/AMF/1881567	Ontario - Turkey Point Mature Deciduous	AmerifluxFLUXNET
CH-Aws	GRA	46.583194	9.790417	https://doi.org/10.18160/2G60-ZHAK	Alp Weissenstein	WarmWinter2020
CH-Cha	GRA	47.210222	8.410444	https://doi.org/10.18160/2G60-ZHAK	Chamau grassland	WarmWinter2020
CH-Dav	ENF	46.815330	9.855910	https://doi.org/10.18160/2G60-ZHAK	Davos	WarmWinter2020
CH-Fru	GRA	47.115833	8.537778	https://doi.org/10.18160/2G60-ZHAK	Fruebuel grassland	WarmWinter2020
CH-Oe1	GRA	47.285833	7.731944	https://doi.org/10.18140/FLX/1440135	Oensingen grassland	FLUXNET2015
CZ-BK1	ENF	49.502129	18.536859	https://doi.org/10.18160/2G60-ZHAK	Bily Kriz forest	WarmWinter2020
CZ-BK2	GRA	49.494430	18.542850	https://doi.org/10.18140/FLX/1440144	Bily Kriz grassland	FLUXNET2015
CZ-Lnz	MF	48.681611	16.946416	https://doi.org/10.18160/2G60-ZHAK	Lanzhot	WarmWinter2020
CZ-RAJ	ENF	49.443724	16.696513	https://doi.org/10.18160/2G60-ZHAK	Rajec	WarmWinter2020
CZ-Stn	DBF	49.035975	17.969900	https://doi.org/10.18160/2G60-ZHAK	Stitna	WarmWinter2020
CZ-wet	WET	49.024650	14.770350	https://doi.org/10.18160/2G60-ZHAK	Trebon	WarmWinter2020
DE-Gri	GRA	50.950040	13.512590	https://doi.org/10.18160/2G60-ZHAK	Grillenburg	WarmWinter2020
DE-Hai	DBF	51.079167	10.453000	https://doi.org/10.18160/2G60-ZHAK	Hainich	WarmWinter2020
DE-HoH	DBF	52.085306	11.219222	https://doi.org/10.18160/2G60-ZHAK	Hohes Holz	WarmWinter2020
DE-Hte	WET	54.210278	12.176111	https://doi.org/10.18160/YVR0-4898	Huetelmoor	ICOSDrought2018
DE-Hzd	DBF	50.963810	13.489780	https://doi.org/10.18160/2G60-ZHAK	Hetzdorf	WarmWinter2020
DE-Lkb	ENF	49.099617	13.304667	https://doi.org/10.18140/FLX/1440214	Lackenberg	FLUXNET2015
DE-Lnf	DBF	51.328217	10.367800	https://doi.org/10.18140/FLX/1440150	Leinefelde	FLUXNET2015
DE-Obe	ENF	50.786660	13.721290	https://doi.org/10.18160/2G60-ZHAK	Oberbärenburg	WarmWinter2020
DE-RuR	GRA	50.621914	6.304126	https://hdl.handle.net/11676/POOKwHoQty8EN0xRHoBbfx28	Rollesbroich	ICOSFLUXNET
DE-Tha	ENF	50.962560	13.565150	https://doi.org/10.18160/2G60-ZHAK	Tharandt	WarmWinter2020

DK-Sor	DBF	55.485869	11.644644	https://doi.org/10.18160/2G60-ZHAK	Soroe	WarmWinter2020
ES-Abr	SAV	38.701839	-6.785881	https://doi.org/10.18160/2G60-ZHAK	Albuera	WarmWinter2020
ES-Agu	OSH	36.940046	-2.033208	https://doi.org/10.18160/2G60-ZHAK	Aguamarga	WarmWinter2020
ES-Amo	OSH	36.833608	-2.252318	https://doi.org/10.18140/FLX/1440156	Amoladeras	FLUXNET2015
ES-LJu	OSH	36.926594	-2.752115	https://doi.org/10.18160/2G60-ZHAK	Llano de los Juanes	WarmWinter2020
ES-LM1	SAV	39.942690	-5.778683	https://doi.org/10.18160/2G60-ZHAK	Majadas del Tietar North	WarmWinter2020
ES-LM2	SAV	39.934592	-5.775881	https://doi.org/10.18160/2G60-ZHAK	Majadas del Tietar South	WarmWinter2020
FI-Hyy	ENF	61.847410	24.294770	https://doi.org/10.18160/2G60-ZHAK	Hyytiala	WarmWinter2020
FI-Let	ENF	60.641830	23.959520	https://doi.org/10.18160/2G60-ZHAK	Lettosuo	WarmWinter2020
FI-Sii	WET	61.832650	24.192850	https://hdl.handle.net/11676/QfuBdfWZTepx1GZ5ot4VOI5h	Siikaneva	ICOSFLUXNET
FI-Sod	ENF	67.362386	26.638591	https://doi.org/10.18140/FLX/1440160	Sodankyla	FLUXNET2015
FI-Var	ENF	67.754900	29.610000	https://doi.org/10.18160/2G60-ZHAK	Varrio	WarmWinter2020
FR-Bil	ENF	44.493672	-0.956082	https://doi.org/10.18160/2G60-ZHAK	Bilos	WarmWinter2020
FR-FBn	MF	43.240790	5.678650	https://doi.org/10.18160/2G60-ZHAK	Font-Blanche	WarmWinter2020
FR-Fon	DBF	48.476358	2.780096	https://doi.org/10.18160/2G60-ZHAK	Fontainebleau-Barbeau	WarmWinter2020
FR-Hes	DBF	48.674100	7.064650	https://doi.org/10.18160/2G60-ZHAK	Hesse	WarmWinter2020
FR-LBr	ENF	44.717110	-0.769300	https://doi.org/10.18140/FLX/1440163	Le Bray	FLUXNET2015
FR-Pue	EBF	43.741300	3.595700	https://doi.org/10.18140/FLX/1440164	Puechabon	FLUXNET2015
GF-Guy	EBF	5.278772	-52.924862	https://doi.org/10.18160/2G60-ZHAK	Guyaflux	WarmWinter2020
GL-NuF	WET	64.130830	-51.386110	https://doi.org/10.18140/FLX/1440222	Nuuk Fen	FLUXNET2015
GL-ZaH	GRA	74.473280	-20.550300	https://doi.org/10.18140/FLX/1440224	Zackenberg Heath	FLUXNET2015
IL-Yat	ENF	31.345045	35.051989	https://doi.org/10.18160/2G60-ZHAK	Yatir	WarmWinter2020
IT-Col	DBF	41.849360	13.588140	https://doi.org/10.18140/FLX/1440167	Collelongo	FLUXNET2015
IT-Cp2	EBF	41.704266	12.357293	https://doi.org/10.18160/2G60-ZHAK	Castelporziano2	WarmWinter2020
IT-Cpz	EBF	41.705249	12.376106	https://doi.org/10.18140/FLX/1440168	Castelporziano	FLUXNET2015
IT-Lav	ENF	45.956200	11.281320	https://doi.org/10.18160/2G60-ZHAK	Lavarone	WarmWinter2020
IT-Lsn	OSH	45.740481	12.750297	https://hdl.handle.net/11676/5b1r2cK2QQxHcZBqbNiF3h_	Lison	ICOSFLUXNET
IT-MBo	GRA	46.014678	11.045831	https://doi.org/10.18160/2G60-ZHAK	Monte Bondone	WarmWinter2020
IT-Noe	CSH	40.606176	8.151169	https://doi.org/10.18140/FLX/1440171	Arca di Noe - Le Prigionette	FLUXNET2015

IT-Ren	ENF	46.586860	11.433690	https://doi.org/10.18160/2G60-ZHAK	Renon	WarmWinter2020
IT-Ro1	DBF	42.408120	11.930010	https://doi.org/10.18140/FLX/1440174	Roccarespampani 1	FLUXNET2015
IT-Ro2	DBF	42.390260	11.920930	https://doi.org/10.18140/FLX/1440175	Roccarespampani 2	FLUXNET2015
IT-SR2	ENF	43.732026	10.290954	https://doi.org/10.18160/2G60-ZHAK	San Rossore 2	WarmWinter2020
IT-SRo	ENF	43.727861	10.284444	https://doi.org/10.18140/FLX/1440176	San Rossore	FLUXNET2015
IT-Tor	GRA	45.844440	7.578055	https://doi.org/10.18160/2G60-ZHAK	Torgnon	WarmWinter2020
MY-PSO	EBF	2.973000	102.306200	https://doi.org/10.18140/FLX/1440240	Pasoh Forest Reserve (PSO)	FLUXNET2015
NL-Hor	GRA	52.240350	5.071301	https://doi.org/10.18140/FLX/1440177	Horstermeer	FLUXNET2015
NL-Loo	ENF	52.166581	5.743556	https://doi.org/10.18160/YVR0-4898	Loobos	ICOSDrought2018
RU-Cok	OSH	70.829139	147.494278	https://doi.org/10.18140/FLX/1440182	Chokurdakh	FLUXNET2015
RU-Fy2	ENF	56.447603	32.901878	https://doi.org/10.18160/2G60-ZHAK	Fyodorovskoye dry spruce stand	WarmWinter2020
RU-Fyo	ENF	56.461528	32.922083	https://doi.org/10.18160/2G60-ZHAK	Fyodorovskoye	WarmWinter2020
SD-Dem	SAV	13.282900	30.478300	https://doi.org/10.18140/FLX/1440186	Demokeya	FLUXNET2015
SE-Deg	WET	64.182029	19.556539	https://doi.org/10.18160/2G60-ZHAK	Degero	WarmWinter2020
SE-Htm	ENF	56.097630	13.418970	https://doi.org/10.18160/2G60-ZHAK	Hyltemossa	WarmWinter2020
SE-Nor	ENF	60.086497	17.479503	https://doi.org/10.18160/2G60-ZHAK	Norunda	WarmWinter2020
SE-Ros	ENF	64.172500	19.738000	https://doi.org/10.18160/2G60-ZHAK	Rosinedal-3	WarmWinter2020
SE-Svb	ENF	64.256110	19.774500	https://doi.org/10.18160/2G60-ZHAK	Svartberget	WarmWinter2020
US-Atq	WET	70.469600	- 157.408900	https://doi.org/10.18140/FLX/1440067	Atqasuk	FLUXNET2015
US-Blo	ENF	38.895300	- 120.632800	https://doi.org/10.18140/FLX/1440068	Blodgett Forest	FLUXNET2015
US-BZB	WET	64.695500	- 148.320800	https://doi.org/10.17190/AMF/1881569	Bonanza Creek Thermokarst Bog	AmerifluxFLUXNET
US-BZF	WET	64.701300	- 148.312100	https://doi.org/10.17190/AMF/1881570	Bonanza Creek Rich Fen	AmerifluxFLUXNET
US-BZS	ENF	64.696300	- 148.323500	https://doi.org/10.17190/AMF/1881572	Bonanza Creek Black Spruce	AmerifluxFLUXNET
US-GLE	ENF	41.366500	- 106.239900	https://doi.org/10.17190/AMF/1871136	GLEES	AmerifluxFLUXNET
US-Goo	GRA	34.254700	-89.873500	https://doi.org/10.18140/FLX/1440070	Goodwin Creek	FLUXNET2015
US-Ho2	ENF	45.209100	-68.747000	https://doi.org/10.17190/AMF/1881581	Howland Forest (west tower)	AmerifluxFLUXNET
US-IB2	GRA	41.840600	-88.241000	https://doi.org/10.18140/FLX/1440072	Fermi National Accelerator Laboratory- Batavia (Prairie site)	FLUXNET2015
US-ICs	WET	68.605800	- 149.311000	https://doi.org/10.17190/AMF/1871138	Imnavait Creek Watershed Wet Sedge Tundra	AmerifluxFLUXNET
US-ICt	OSH	68.606300	- 149.304100	https://doi.org/10.17190/AMF/1881583	Imnavait Creek Watershed Tussock Tundra	AmerifluxFLUXNET

US-Jo2	OSH	32.584900	-106.603200	https://doi.org/10.17190/AMF/1881584	Jornada Experimental Range Mixed Shrubland	AmerifluxFLUXNET
US-KFS	GRA	39.056100	-95.190700	https://doi.org/10.17190/AMF/1881585	Kansas Field Station	AmerifluxFLUXNET
US-KLS	GRA	38.774500	-97.568400	https://doi.org/10.17190/AMF/1854367	Kansas Land Institute	AmerifluxFLUXNET
US-Los	WET	46.082700	-89.979200	https://doi.org/10.18140/FLX/1440076	Lost Creek	FLUXNET2015
US-Me2	ENF	44.452300	-121.557400	https://doi.org/10.17190/AMF/1854368	Metolius mature ponderosa pine	AmerifluxFLUXNET
US-Me3	ENF	44.315400	-121.607800	https://doi.org/10.17190/AMF/1902835	Metolius-second young aged pine	AmerifluxFLUXNET
US-Me6	ENF	44.323300	-121.607800	https://doi.org/10.18140/FLX/1440099	Metolius Young Pine Burn	FLUXNET2015
US-MOz	DBF	38.744100	-92.200000	https://doi.org/10.17190/AMF/1854370	Missouri Ozark Site	AmerifluxFLUXNET
US-Mpj	WSA	34.438400	-106.237700	https://doi.org/10.17190/AMF/1832161	Mountainair Pinyon-Juniper Woodland	AmerifluxFLUXNET
US-NC1	OSH	35.811800	-76.711900	https://doi.org/10.17190/AMF/1902836	NC_Clearcut	AmerifluxFLUXNET
US-NC4	WET	35.787900	-75.903800	https://doi.org/10.17190/AMF/1902837	NC_AlligatorRiver	AmerifluxFLUXNET
US-NR1	ENF	40.032900	-105.546400	https://doi.org/10.17190/AMF/1871141	Niwot Ridge Forest (LTER NWT1)	AmerifluxFLUXNET
US-Oho	DBF	41.554500	-83.843800	https://doi.org/10.18140/FLX/1440088	Oak Openings	FLUXNET2015
US-ONA	GRA	40.177600	-112.452400	https://doi.org/10.17190/AMF/1832163	Florida pine flatwoods	AmerifluxFLUXNET
US-Ro4	GRA	44.678100	-93.072300	https://doi.org/10.17190/AMF/1881589	Rosemount Prairie	AmerifluxFLUXNET
US-Seg	GRA	34.362300	-106.701900	https://doi.org/10.17190/AMF/1984572	Sevilleta grassland	AmerifluxFLUXNET
US-Ses	OSH	34.334900	-106.744200	https://doi.org/10.17190/AMF/1984573	Sevilleta shrubland	AmerifluxFLUXNET
US-SRC	OSH	31.908300	-110.839500	https://doi.org/10.18140/FLX/1440098	Santa Rita Creosote	FLUXNET2015
US-SRG	GRA	31.789400	-110.827700	https://doi.org/10.18140/FLX/1440114	Santa Rita Grassland	FLUXNET2015
US-SRM	WSA	31.821400	-110.866100	https://doi.org/10.18140/FLX/1440090	Santa Rita Mesquite	FLUXNET2015
US-Syv	MF	46.242000	-89.347700	https://doi.org/10.18140/FLX/1440091	Sylvania Wilderness Area	FLUXNET2015
US-Ton	WSA	38.431600	-120.966000	https://doi.org/10.18140/FLX/1440092	Tonzi Ranch	FLUXNET2015
US-Var	GRA	38.413300	-120.950700	https://doi.org/10.17190/AMF/1993904	Vaira Ranch- Ione	AmerifluxFLUXNET
US-WCr	DBF	45.805900	-90.079900	https://doi.org/10.18140/FLX/1440095	Willow Creek	FLUXNET2015
US-Whs	OSH	31.743800	-110.052200	https://doi.org/10.17190/AMF/1984574	Walnut Gulch Lucky Hills Shrub	AmerifluxFLUXNET
US-Wkg	GRA	31.736500	-109.941900	https://doi.org/10.17190/AMF/1984575	Walnut Gulch Kendall Grasslands	AmerifluxFLUXNET
US-xBR	DBF	44.063900	-71.287300	https://doi.org/10.17190/AMF/1881598	NEON Bartlett Experimental Forest (BART)	AmerifluxFLUXNET
US-xCL	GRA	33.401200	-97.570000	https://doi.org/10.17190/AMF/1985435	NEON LBJ National Grassland (CLBJ)	AmerifluxFLUXNET
US-xDC	GRA	47.161700	-99.106600	https://doi.org/10.17190/AMF/1985437	NEON Dakota Coteau Field School (DCFS)	AmerifluxFLUXNET

US-xHA	DBF	42.536900	-72.172700	https://doi.org/10.17190/AMF/1985441	NEON Harvard Forest (HARV)	AmerifluxFLUXNET
US-xJE	ENF	31.194800	-84.468600	https://doi.org/10.17190/AMF/1985443	NEON Jones Ecological Research Center (JERC)	AmerifluxFLUXNET
US-xKZ	GRA	39.100800	-96.563100	https://doi.org/10.17190/AMF/1985445	NEON Konza Prairie Biological Station (KONZ)	AmerifluxFLUXNET
US-xSB	ENF	29.689300	-81.993400	https://doi.org/10.17190/AMF/1985451	NEON Ordway-Swisher Biological Station (OSBS)	AmerifluxFLUXNET
US-xSE	DBF	38.890100	-76.560000	https://doi.org/10.17190/AMF/1985452	NEON Smithsonian Environmental Research Center (SERC)	AmerifluxFLUXNET
US-xST	DBF	45.508900	-89.586400	https://doi.org/10.17190/AMF/1985454	NEON Steigerwaldt Land Services (STEI)	AmerifluxFLUXNET
US-xTR	DBF	45.493700	-89.585700	https://doi.org/10.17190/AMF/1985456	NEON Treehaven (TREE)	AmerifluxFLUXNET
US-xUK	DBF	39.040400	-95.192100	https://doi.org/10.17190/AMF/1985457	NEON The University of Kansas Field Station (UKFS)	AmerifluxFLUXNET
US-xUN	MF	46.233900	-89.537300	https://doi.org/10.17190/AMF/1985458	NEON University of Notre Dame Environmental Research Center (UNDE)	AmerifluxFLUXNET
ZM-Mon	WSA	-15.437778	23.252778	https://doi.org/10.18140/FLX/1440189	Mongu	FLUXNET2015

Table S3. Eddy-covariance variables used for the calculation of the ecosystem functional properties and for the calculation of meteorological predictors used in the analyses.

Variable	Variable name	Units	Additional details
ET	Evapotranspiration	mmol H_20 m^{-2} s^{-1}	Calculated from LE and TA as LE / (2.501 - 0.00236 * TA) * 18.016 with the *fCalcETfromLE* function of the *REddyProc* R package[1]
GPP_NT	Gross primary productivity	µmol CO^2 m^{-2} s^{-1}	From Nighttime partitioning method, 50^{th} percentile calculated from the 40 estimates
H	Sensible heat flux	W m^{-2}	Gap-filled using MDS method[2]
LE	Latent heat flux	W m^{-2}	Gap-filled using MDS method[2]
NEE	Net ecosystem exchange	µmol CO^2 m^{-2} s^{-1}	NEE VUT 50^{th} percentile calculated from the 40 estimates
NETRAD	Net radiation	W m^{-2}	
PA	Atmospheric pressure	kPa	
PPFD	Photosynthetic photon flux density	W m^{-2}	Calculated as SWin * 2.11[3]
P	Precipitation	mm h^{-1}	
RECO_NT	Ecosystem respiration	µmol CO^2 m^{-2} s^{-1}	From Nighttime partitioning method, 50^{th} percentile calculated from the 40 estimates
RH	Relative humidity	%	
SW_IN	Shortwave incoming radiation	W m^{-2}	Gap-filled using MDS method[2]. Negative values set to zero - e.g.: negative values from instrumentation noise
TA	Air Temperature	°C	Gap-filled using MDS method[2]
USTAR	Friction velocity	m s^{-1}	
VPD	Vapor pressure deficit	hPa	Gap-filled using MDS method[2]
WS	Wind speed	m s^{-1}	

References

1. Wutzler, T. *et al.* Basic and extensible post-processing of eddy covariance flux data with REddyProc. *Biogeosciences* **15**, 5015–5030 (2018).
2. Reichstein, M. *et al.* On the separation of net ecosystem exchange into assimilation and ecosystem respiration: review and improved algorithm. *Global Change Biology* **11**, 1424–1439 (2005).
3. Britton, C. M. & Dodd, J. D. Relationships of photosynthetically active radiation and shortwave irradiance. *Agricultural Meteorology* **17**, 1–7 (1976).